

Net Shortwave Fluxes over the Ocean

JAMES D. SCOTT AND MICHAEL A. ALEXANDER

CIRES, Boulder, Colorado

5 October 1998 and 29 June 1999

ABSTRACT

Net surface shortwave fluxes (Q_{sw}) computed from National Aeronautics and Space Administration/Langley satellite data are compared with Q_{sw} from reanalyses of the European Centre for Medium-Range Weather Forecasts (ERA) and the National Centers for Environmental Prediction (NCEP). The mean and variability of Q_{sw} is examined for the period 1983–91, with a focus on the tropical and summer hemisphere oceans during June, July, August (JJA) and December, January, February (DJF). Both reanalyses exhibit a positive bias, indicating too much sunlight is absorbed at the surface, in regions where low-level stratiform clouds are most common, but a negative bias in regions where cumuliform clouds are the dominant cloud type. The ERA has a greater intermonthly variability during JJA than the satellite data over most of the Pacific, especially north of 40°N and in the central and eastern equatorial Pacific. The NCEP variability in JJA is also larger than the satellite estimates over the North Pacific and the eastern equatorial Pacific, but is smaller over most of the western tropical and subtropical Pacific. During DJF, the ERA has more realistic variability in shortwave fluxes over the tropical oceans than the NCEP reanalysis, which underestimates the variability in the tropical Pacific and the Indian Ocean by a factor of 2. Ocean models using atmospheric forcing from reanalyses will be impacted not only by regional and seasonal Q_{sw} biases but also by differences in Q_{sw} variability. It is estimated that the largest impacts on SST due to differences in variability are in the North Pacific, eastern tropical Pacific, and western Atlantic during JJA and in the Indian Ocean and the tropical Pacific and Atlantic during DJF.

1. Introduction

In recent years there has been an effort to establish accurate estimates of the earth's surface radiation budget (SRB) and to assess the impact that the individual components of the budget have on climate. Since long-term surface measurements of radiative fluxes are limited primarily to continental regions (Ohmura and Gilgen 1991), satellite estimates of cloudiness and top of the atmosphere fluxes have been used in conjunction with radiative transfer models to produce global estimates of the SRB (Li 1995; Rossow and Zhang 1995; Whitlock et al. 1995; Gupta et al. 1997). The most common algorithms used in computing SRB estimates from satellite data, Pinker (Pinker and Lazo 1992) and Staylor (Darnell et al. 1992), were validated by Whitlock et al. (1995) using Global Energy Budget Archive (GEBA) surface measurements (Ohmura and Gilgen 1991) for the period of 1985–88. Over oceanic regions, the satellite bias relative to GEBA measurements is 0–15 W m⁻² for both the Pinker and Staylor algorithms. Biases

are largest for cells containing coastlines, mountainous topography, highly reflective surfaces such as sea ice or deserts, and poleward of 60°. Ward (1995) found the Pinker SRB to have larger bias and rms differences over the Tropics (15 W m⁻², 35 W m⁻²) than the midlatitudes (5 W m⁻², 15 W m⁻²) when compared with GEBA measurements. Gupta et al. (1997), who used the Staylor algorithm on satellite data from 1983 to 1991, performed a surface validation and found an overall bias of 5 W m⁻² and an rms difference of 24 W m⁻². The latter dataset is used in the present study for comparison with two reanalysis datasets.

Satellite datasets have also been used to assess how well the SRB is represented by atmospheric general circulation models (AGCMs) since radiative fluxes are believed to play a critical role in climate change (Ward 1995; Cess et al. 1997; Garret et al. 1998). Cess et al. (1997) performed a comprehensive comparison of cloud radiative forcing in AGCMs with satellite estimates and found rms differences to be larger for shortwave cloud forcing (SWCF) compared to longwave cloud forcing (LWCF) in 14 out of 18 AGCMs. Garret et al. (1998), report that recent improvements to AGCMs have reduced biases seen in earlier versions of the same models, but systematic overestimation of the downwelling shortwave flux persists and contributes to positive biases in the net surface radiation.

Corresponding author address: Mr. James D. Scott, Cooperative Institute for Research in Environmental Sciences, NOAA Climate Diagnostics Center, R/E/CD1, 325 Broadway, Boulder, CO 80303-3328.
E-mail: jds@cdc.noaa.gov

Global reanalyses such as the National Centers for Environmental Prediction (NCEP) (Kalnay et al. 1996), National Aeronautics and Space Administration/Data Assimilation Office (NASA/DAO) (Schubert et al. 1993), and the European Centre for Medium-Range Weather Forecasts Reanalysis (ERA 1998) projects have provided climate researchers with alternative estimates of the earth's SRB. Reanalyses contain continuous time series of atmospheric variables under one data assimilation system, facilitating comparison of climate anomalies in different years without the biases introduced by changes in the data assimilation scheme. While some variables are highly constrained by the observations used in the assimilation (e.g., temperature, winds, pressure), other variables are not, and therefore are subject to the typical biases found in AGCMs. Clouds, precipitation, and shortwave and longwave radiation are only constrained by the observations to the extent that the winds, temperature, etc., affect their prediction in the model.

Weare (1997) and Bony et al. (1997) have compared SRB variables in NASA/DAO and NCEP reanalyses with satellite estimates. Weare (1997) examined cloud forcing from the NCEP reanalysis and those derived from the Earth Radiation Budget Experiment (ERBE) and noted the annual mean bias in the NCEP SWCF was of largest magnitude ($< -40 \text{ W m}^{-2}$) in the Tropics and subtropics. By examining August 1988–August 1987 differences in SWCF, Weare (1997) found the largest discrepancies between the NCEP and ERBE data over the tropical western Pacific. Bony et al. (1997) used data from the NASA/DAO and NCEP reanalyses for the period 1987–88 to compare net shortwave radiation at the surface (Q_{sw}) (among other variables) to satellite estimates in the Tropics (30°S–30°N). They found annual mean biases in NCEP Q_{sw} over the tropical ocean ranged from -10 to -30 W m^{-2} , while NASA/DAO Q_{sw} biases ranged from $+50 \text{ W m}^{-2}$ in subsidence regions of the subtropics to -25 W m^{-2} in convective regions near the equator. Bony et al. (1997) also examined interannual changes by comparing 1987 to 1988 anomalies and concluded that the DAO reanalysis overestimated the interannual variability in SWCF by a factor of 2 in the tropical Pacific, while the NCEP SWCF had lower amplitude variability in the western tropical Pacific and higher amplitude variability in the eastern tropical Pacific relative to the observations.

In this paper, we expand upon the work of Weare (1997) and Bony et al. (1997) by comparing the Q_{sw} in the NCEP reanalysis and the ERA to the NASA/Langley satellite (NLS) estimates (Gupta et al. 1997). Since our focus is on how differences in these datasets could impact ocean modeling efforts, we examine Q_{sw} statistics over the tropical and summer hemisphere oceans. During summer SWCF is a maximum in the middle latitudes and the oceanic mixed layer depth is relatively shallow, making the SST more sensitive to changes in Q_{sw} . By using 24 months of data, we also can make more ac-

curate statistical inferences of the bias and intermonthly variability of Q_{sw} in the three datasets. We will show that not only are there substantial differences in Q_{sw} in the Tropics as has been found in the studies cited above, but significant regional differences at higher latitudes when one examines seasonal averages as opposed to annual averages. We also assess where these differences in shortwave fluxes may lead to the largest modification of the SST. Furthermore, the ERA (1999) is a relatively recent dataset and so it is worth evaluating its estimates of Q_{sw} .

2. Data and methods

Monthly means of net shortwave radiation at the surface are constructed from the four times daily data in the NCEP (Kalnay et al. 1996) and ERA (ERA 1999) reanalysis data for June, July, and August (JJA) and December, January, February (DJF) during the period July 1983 to June 1991, the same period for which the NLS (Gupta et al. 1997) satellite data are available. The NCEP and NLS data are interpolated to a common $2.5^\circ \times 2.5^\circ$ grid (the same grid as ERA) for comparison. The statistical significance of the biases is assessed using the Student's *t*-test with a pooled estimate of variance and the significance of the ratios of standard deviations is assessed using a two-tailed *F* distribution (Snedecor and Cochran 1980). The standard deviations are computed using monthly anomalies. The observed mixed layer depths used to estimate the SST impact due to differences in the shortwave forcing are from Monterey and Levitus (1997).

3. Net shortwave fluxes

The Q_{sw} estimates from the satellite data for JJA are shown in Fig. 1a. The relatively low values for satellite estimated Q_{sw} during JJA north of 40°N (Fig. 1a) are primarily associated with large amounts of stratiform clouds (Warren et al. 1988) generated by extratropical cyclones (Weaver and Ramanathan 1996). The subtropical North Pacific, a relatively cloud free region due to large-scale descent and a relatively stable boundary layer, has the highest Q_{sw} , with a maximum near the Hawaiian Islands ($>280 \text{ W m}^{-2}$). Farther to the east, between 20°–30°N the low-level flow is more northerly, which advects relatively cool air over warmer water. Cold air advection, combined with large-scale descent acts to produce a marine stratocumulus layer, which in turn is responsible for the relative minimum in Q_{sw} (Klein and Hartmann 1993). There is also a relatively cloud free region due to large-scale descent and stability in the boundary layer in the central North Atlantic. From 8° to 10°N throughout the Pacific and the Atlantic, a relative minimum in Q_{sw} is representative of the deep convection in the intertropical convergence zone (ITCZ). Farther south, near the coast of Peru in the Pacific and Namibia in the Atlantic, regions dominated by marine

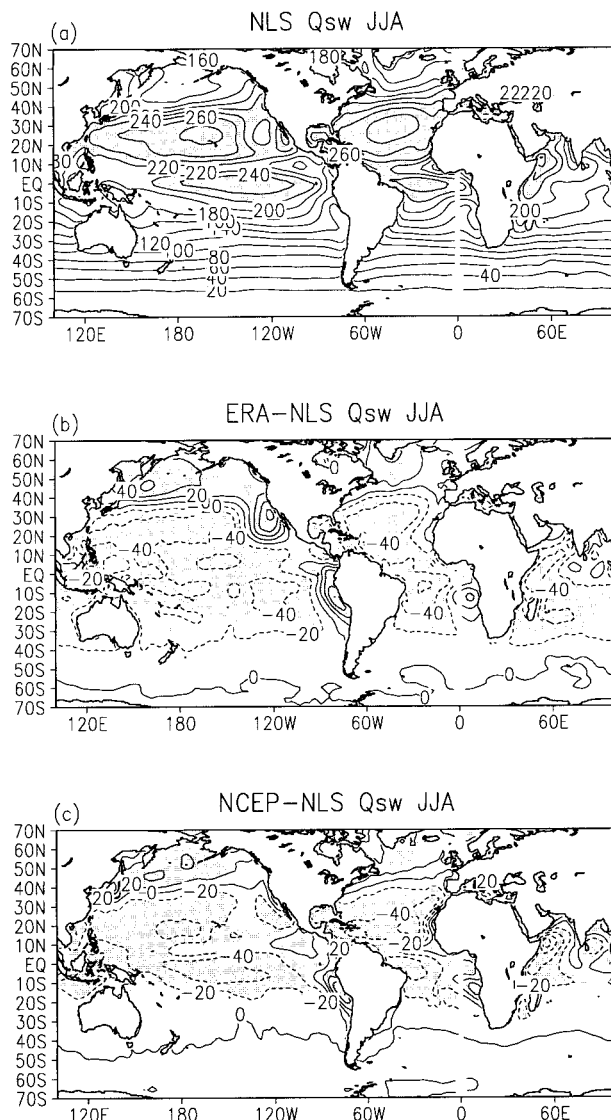


FIG. 1. (a) NLS Q_{sw} for JJA (Jul 1983–Jun 1991). Contour interval is 20 W m^{-2} , shading indicates values >220 . (b) ERA – NLS Q_{sw} bias for JJA. Contour interval is 20 W m^{-2} , shading indicates 99% significance limit. (c) Same as (b) except NCEP – NLS bias.

stratus (Warren et al. 1988; Klein and Hartmann 1993), Q_{sw} is $20\text{--}50 \text{ W m}^{-2}$ less than other parts of the Pacific at the same latitude.

The JJA bias in Q_{sw} for the ERA is shown in Fig. 1b. A positive bias, indicative of too much sunlight absorbed at the surface, exists in most of the north and eastern Pacific with three regions showing differences that are significant within a 99% confidence limit: the North Pacific north of 40°N and the subtropical regions near California and Peru in the Pacific. The Q_{sw} bias exceeds 60 W m^{-2} in each of these regions and 80 W m^{-2} near Baja California. These regions coincide with areas observed to have $>50\%$ stratus coverage during JJA (Warren et al. 1988; Klein and Hartmann 1993).

The bias over the Atlantic Ocean is similar to the Pacific, in that the northern and eastern portions of the basin have positive bias, yet the magnitudes are not as large as in the Pacific. The two significant regions of positive bias in the Atlantic are south of Greenland and near Namibia, regions also dominated by stratiform clouds during JJA. The remaining portions of the tropical and subtropical oceans exhibit a negative Q_{sw} bias that is statistically significant, with magnitudes ranging from -20 to -50 W m^{-2} . The Warren et al. (1988) atlas indicates these are relatively stratus free ($<20\%$) regions.

The Q_{sw} bias in the NCEP data (Fig. 1c) for the same period is, with a few exceptions, quite similar to ERA (Fig. 1b). There is a significant positive bias north of 40°N and near the coasts of Peru and Namibia, but in contrast to ERA, the NCEP bias is negative near the stratocumulus region off the coast of California. The NCEP bias is significantly negative throughout the tropical and subtropical oceans except for a small window near 10°N where the bias is not significant at the 99% level. The magnitude of the NCEP bias is smaller than or comparable to that of the ERA over most of the Pacific and Atlantic Oceans, while the negative bias has a larger magnitude in the Indian Ocean. This is likely a result of the NCEP bias being smaller than the ERA due to compensating errors. The NCEP data underestimate total cloud fraction while overestimating cloud albedo (Bony et al. 1997; Weare 1997).

The Q_{sw} estimates from the satellite data for DJF for the Tropics and the Southern Hemisphere are shown in Fig. 2a. The satellite estimates of Q_{sw} are largest ($>300 \text{ W m}^{-2}$) in the subtropical latitudes of the South Pacific and Atlantic Oceans, where the cloud-free centers of seasonal high pressure circulations are typically located. In the Pacific Ocean, the Q_{sw} is smaller to the east and west of the subtropical high pressure center (25°S , 110°W). To the west, the shortwave flux is reduced by the deep convective clouds in the South Pacific convergence zone (SPCZ). To the east, near the coast of Peru, low-level stratus is predominant (Klein and Hartmann 1993; Warren et al. 1988). In the Atlantic Ocean, low clouds are also predominant near the coast of Africa, resulting in decreased Q_{sw} . To the west of the subtropical high in the Atlantic, Q_{sw} is reduced by convective clouds in the South Atlantic convergence zone (SACZ). The Q_{sw} field is largely zonal farther south, as there are fewer landmasses to influence the atmospheric circulation.

The Q_{sw} bias for ERA in the southern oceans during DJF (Fig. 2b) is similar to the ERA bias in the northern oceans during JJA (Fig. 1b) in that the bias is positive in the eastern subtropical Atlantic and Pacific Oceans and poleward of 40° . Additionally, the regions with positive biases that are statistically significant within a 99% confidence limit are regions where low-level clouds are the dominant cloud type (Warren et al. 1988). Positive biases exceed 60 W m^{-2} in the eastern Pacific and the southern storm track. Most of the Tropics and subtrop-

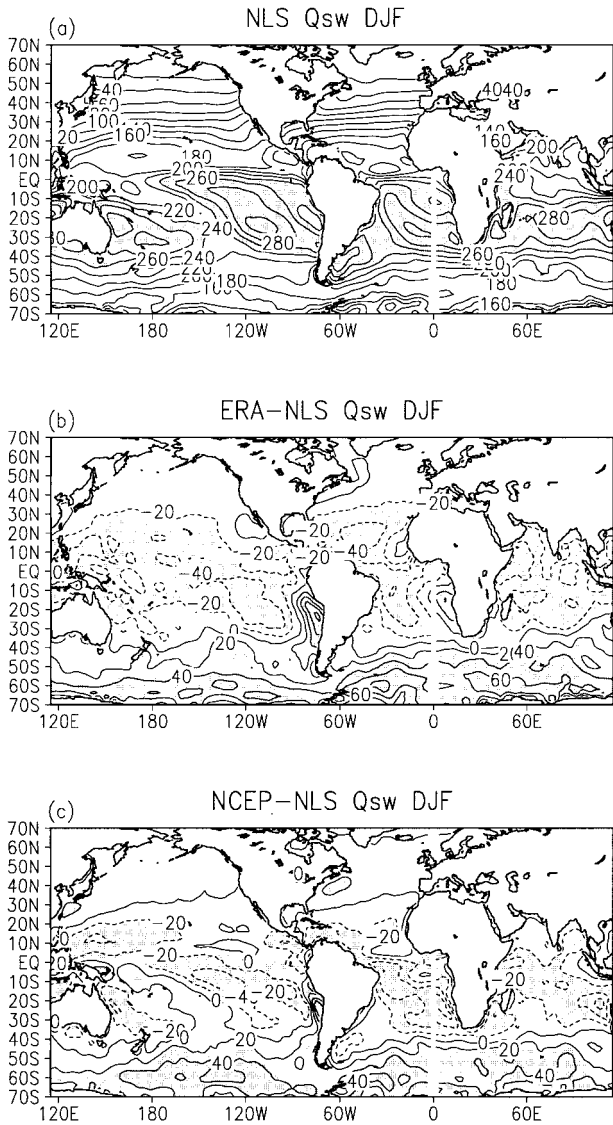


FIG. 2. Same as Fig. 1 except for DJF. Shading in (a) indicates values >240 .

ics, including the Indian Ocean, have bias in the range of -20 to -40 W m^{-2} .

The bias for the NCEP Q_{sw} during the southern summer (Fig. 2c) also indicates too much sunlight being absorbed at the surface near Peru at 25°S , and in the southern storm track, with magnitudes comparable to the ERA bias (Fig. 2b). In contrast to the ERA in JJA and DJF (Figs. 1b, 2b) and the NCEP bias in JJA (Fig. 1c), the DJF bias near Namibia is negative. Also in contrast to the ERA (Fig. 2b), there is a weak positive bias in the region of the SPCZ, perhaps an indication of the convection being underestimated in this region. As in the ERA, the majority of the tropical and subtropical oceans have a bias of -20 to -40 W m^{-2} .

The intermonthly standard deviations (computed from 24 monthly deviations during JJA) of the satellite

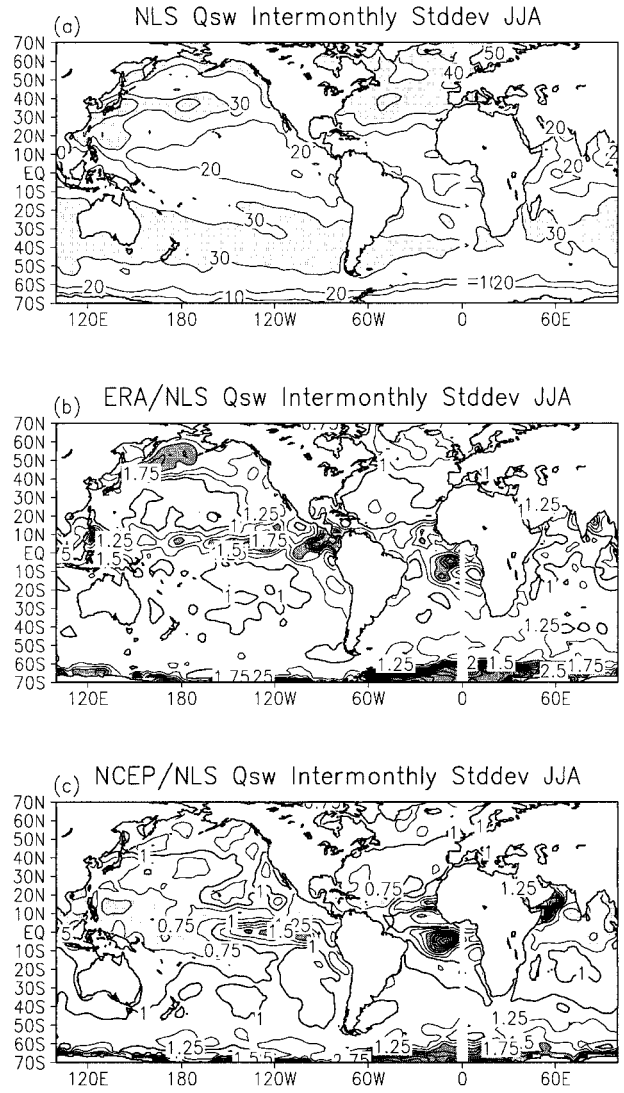


FIG. 3. (a) σ_{NLS} for JJA (Jul 1983–Jun 1991). Contour interval is 5 W m^{-2} , shading indicates values >30 . (b) The $\sigma_{\text{ERA}}/\sigma_{\text{NLS}}$ for JJA. Light (dark) shading indicates standard deviations that are significantly smaller (larger) than σ_{NLS} at the 99% level. (c) Same as (b), except it is the ratio of $\sigma_{\text{NCEP}}/\sigma_{\text{NLS}}$.

estimated $Q_{\text{sw}}(\sigma_{\text{NLS}})$ are shown in Fig. 3a. The largest values of σ_{NLS} for JJA are near Japan and cover most of the coastal areas of the North Pacific. From 30° to 40°N a band of $\sigma_{\text{NLS}} >30 \text{ W m}^{-2}$ extends from Japan eastward to 140°W ; this is a region of climatologically large meridional gradients in SST and stratiform cloud fraction (Warren et al. 1988; Norris and Leovy 1994). Observational studies, such as Weare (1994), Norris and Leovy (1994), and Klein et al. (1995), have shown significant negative correlations between low-level cloudiness and SST on seasonal and interannual timescales in this region. Shifts in the amount of low-level clouds, possibly related to shifts in the southern extent of storm track activity, are likely responsible for the large σ_{NLS}

from 30° to 40°N. A similar process is likely responsible for the large variability in the middle latitudes of the Atlantic Ocean, where standard deviations exceed 35 $W m^{-2}$. The σ_{NLS} is generally less than 25 $W m^{-2}$ between 40° and 50°N in the western Pacific and most of the Tropics and subtropics where intermonthly changes in clouds are less dramatic.

Figures 3b and 3c show the ratios of the ERA and the NCEP intermonthly standard deviations of Q_{sw} (σ_{ERA} and σ_{NCEP}) to the σ_{NLS} for JJA. The σ_{ERA} is greater than σ_{NLS} over most of the Pacific and Atlantic Oceans. A two-tailed F distribution indicates σ_{ERA} is significantly greater than σ_{NLS} (within a 99% confidence limit) in the core of the midlatitude storm track region (40°–50°N), over the central and eastern equatorial Pacific, the eastern tropical Atlantic, and the higher latitudes of the southern oceans. Figure 3c shows that σ_{NCEP} is significantly larger than σ_{NLS} in the eastern equatorial Pacific and Atlantic but smaller over most of the western tropical and subtropical Pacific, the Caribbean Sea, and most of the Indian Ocean. With the exception of the eastern equatorial Atlantic and the northwestern Indian Ocean, σ_{NCEP} is generally smaller than σ_{ERA} .

The σ_{NLS} for DJF, shown in Fig. 4a, indicates zonal gradations in shortwave variability along the equator with maxima ($>30 W m^{-2}$) near the date line and at 90°E. The large variations in Q_{sw} in these regions reflect changes in convective patterns associated with El Niño–Southern Oscillation (ENSO). Just south of the equatorial maximum in the Pacific is a minimum in Q_{sw} variability collocated with the mean position of the convection in the SPCZ. This indicates the core of the convection in the SPCZ does not change location or intensity much during DJF. The flanks of the SPCZ (to the NE and SW) show relative maxima in σ_{NLS} , where the edge of the convection may shift on seasonal to interannual timescales. In the tropical Atlantic the variability is relatively small except for a maximum ($>35 W m^{-2}$) in the South Atlantic convergence zone ($\sim 20^\circ S$ in the western Atlantic Ocean). This region is known to have high convective variability on subseasonal time scales and to a lesser degree on ENSO timescales (Liebmann et al. 1999).

Figures 4b and 4c show the ratios of σ_{ERA} and σ_{NCEP} to the σ_{NLS} for DJF. Over the tropical Pacific, the ERA variability (Fig. 4b) agrees more with the satellite observations than the NCEP Q_{sw} variability (Fig. 4c). While both the σ_{ERA} and σ_{NCEP} data show a maximum variability farther east than σ_{NLS} , the NCEP data have standard deviations less than half the magnitude of the observations along the equator from 150°E to 150°W, which is significant at the 99% level. Along the SPCZ, the ERA variability is enhanced and the NCEP variability is suppressed relative to the satellite estimates. The NCEP standard deviations of Q_{sw} are also significantly weaker than σ_{NLS} in the eastern Indian Ocean. In higher latitudes, both reanalyses have larger standard

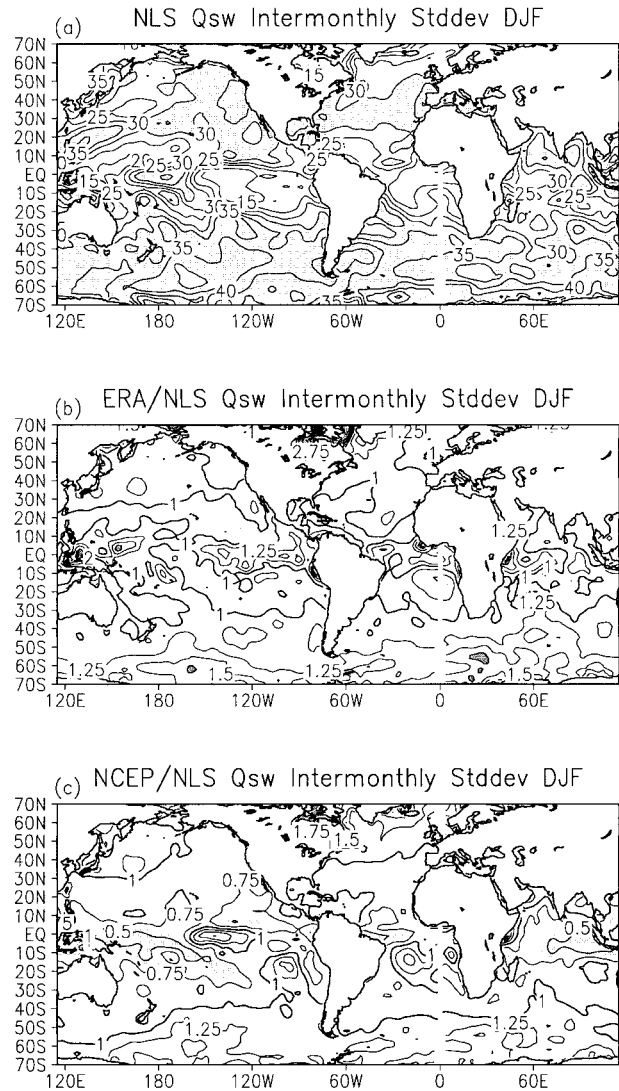


FIG. 4. Same as Fig. 3 except for DJF.

deviations than observed, especially south of 50°S, with ERA having larger values than NCEP.

4. SST impacts

The previous section documented the differences in net shortwave fluxes in the ERA and NCEP reanalyses relative to NLS observations. Now we will estimate the impact errors in Q_{sw} could have on a simple mixed layer ocean model. Since shortwave fluxes are largely absorbed by the oceanic mixed layer, areas with shallow mixed layers are going to be more sensitive, in terms of SST change, to errors in shortwave fluxes. One can estimate the change in mixed layer temperature over a season via

$$\Delta T \propto \frac{\Delta Q \Delta t}{\rho C_H H}, \quad (1)$$

where ΔT is the change in mixed layer temperature ($^{\circ}\text{C}$), ΔQ is the heat flux bias (W m^{-2}), Δt is the number of seconds in the season, ρ is the density of seawater ($1024.438 \text{ kg m}^{-3}$), C_H is the specific heat of seawater ($3950 \text{ J }^{\circ}\text{C}^{-1} \text{ kg}^{-1}$), and H is the mixed layer depth (m) from monthly observation (Monterey and Levitus 1997). The SST errors computed from the above equation using the bias in the Q_{sw} from the reanalyses (Figs. 1 and 2) are rather large, ranging from $\pm 2^{\circ}$ – 5°C over about 30% of the grid points with some isolated areas as large as $\pm 10^{\circ}\text{C}$, assuming no feedbacks from the ocean to the atmosphere (not shown). In ocean modeling, Q_{sw} biases can largely be accounted for with a heat flux correction; yet errors in Q_{sw} intermonthly variability cannot and contribute to significant errors in SST. The rms SST errors are computed via

$$\epsilon_{\text{SST}} = \left[\frac{1}{N-1} \sum_{N=1}^{N=24} \left(\frac{(Q'_{\text{rean}} - Q'_{\text{sat}})\Delta t}{\rho C_H H} \right)^2 \right]^{1/2}, \quad (2)$$

where Q'_{rean} is the monthly anomaly in Q_{sw} from either ERA or NCEP, Q'_{sat} is the monthly anomaly in Q_{sw} from the satellite data, N is the number of months, Δt is the number of seconds in a month; ρ , C_H , and H are defined in Eq. (1).

For a typical month during JJA ϵ_{SST} is shown in Fig. 5. Both ERA (Fig. 5a) and NCEP (Fig. 5b) show $\epsilon_{\text{SST}} > 0.5^{\circ}\text{C}$ in similar regions, primarily where climatological mixed layer depths are less than 30 m (not shown). The ERA has larger rms errors (Fig. 5c) than NCEP over much of the North Pacific, eastern tropical Pacific, and the tropical Atlantic with the largest differences ($>1^{\circ}\text{C}$) along 10°N . The NCEP errors are larger than ERA in the extreme western subtropical Pacific and Atlantic and along the equator. Regions where $\epsilon_{\text{SST}} > 0.5^{\circ}\text{C}$ during DJF (Fig. 6) are also similar for ERA (Fig. 6a) and NCEP (Fig. 6b) and are generally located where the mixed layers are shallow and sensitive to errors in Q_{sw} . The most notable differences (Fig. 6c) between the two reanalyses occur in the eastern tropical Pacific and the tropical Atlantic (where ERA $>$ NCEP) and in the Indian Ocean (where ERA $>$ NCEP in the south and NCEP $>$ ERA in the north).

The SST error estimates do not account for feedbacks that may be present when using these fluxes to force an ocean model. In a model where the mixed layer depth is predicted, too much sunlight could lead to shoaling of the mixed layer which would warm the SST even more. There could also be negative feedbacks if the predicted SST is used to compute latent and sensible heat fluxes instead of using the fluxes output from the reanalysis. The SST impact would be more complicated for an experiment that used the surface flux forcing to drive an ocean general circulation model, where regional biases or rms errors of Q_{sw} could alter SST gradients and therefore oceanic heat transport.

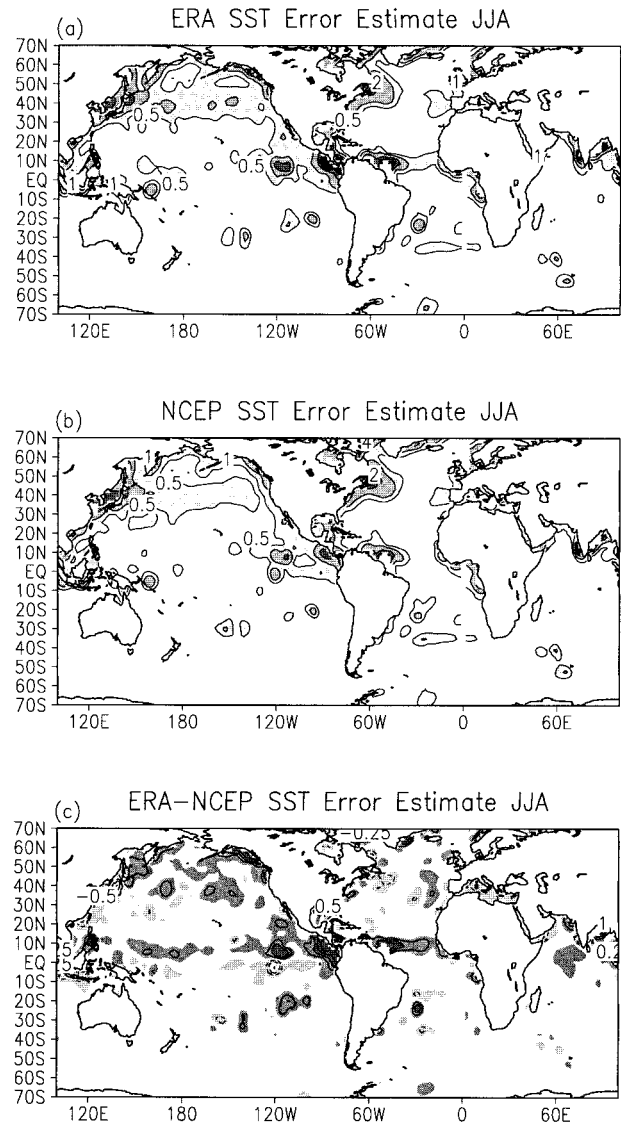


FIG. 5. SST error estimates due to rms errors in Q_{sw} for (a) ERA and (b) NCEP reanalysis for JJA. Contour interval is 0.5°C for values $<1^{\circ}\text{C}$ and 1°C for values $>1^{\circ}\text{C}$. (c) Shows ERA – NCEP SST error differences. Contour levels are ± 0.25 , 0.5 , 1 , 2°C . Dark (light) shading indicates values >0.1 (<-0.1) $^{\circ}\text{C}$. Darkest (lightest) shading indicates values >0.5 (<-0.5) $^{\circ}\text{C}$.

5. Discussion

We have shown how net shortwave flux estimates from the ERA and NCEP reanalysis differ in the first and second moments relative to satellite estimates and how these errors can impact SST. There appear to be several factors that contribute to the discrepancies between satellite and reanalysis shortwave fluxes.

In both the ERA and NCEP data, the regions where the Q_{sw} bias is positive (too much sunlight absorbed at the surface), are regions where low-level stratiform clouds are the dominant cloud type (Warren et al. 1988; Klein and Hartmann 1993). In these regions, ERA and

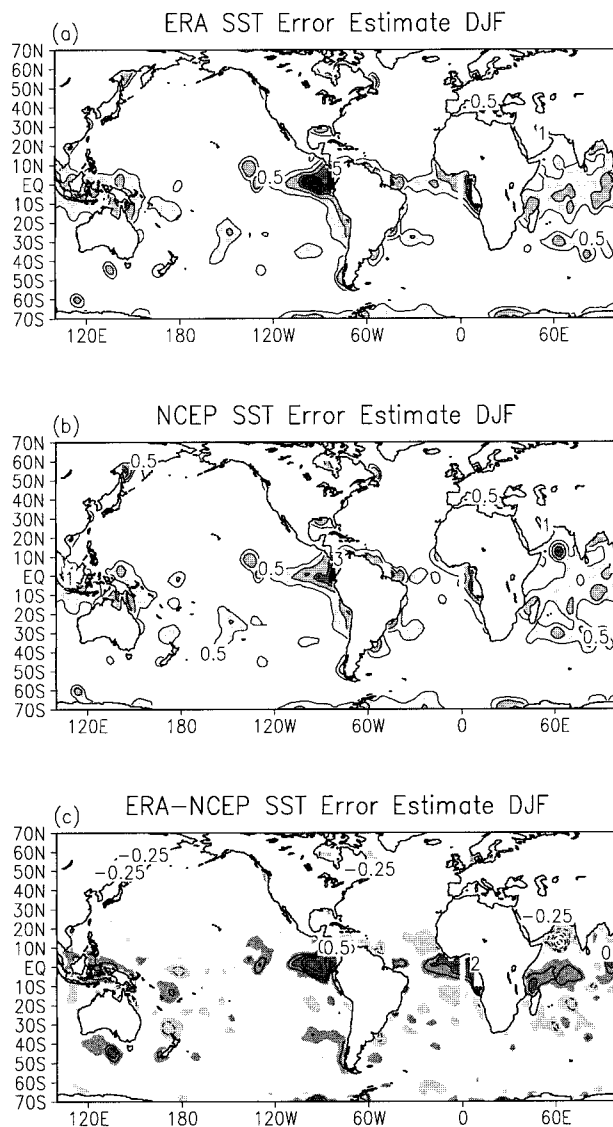


FIG. 6. Same as Fig. 5 except for DJF.

NCEP have less total cloud fraction than in observations (not shown). However, there are two exceptions in the NCEP data, where the Q_{sw} bias < 0 in regions where low-level stratiform cloudiness is predominant: near the Californian coast during JJA and near the Namibian coast in DJF. In these two cases, the NCEP total cloud fraction biases are positive (not shown). Previous studies (Bony et al. 1997; Weare 1997) have shown that cloud albedos are too large in the NCEP reanalysis, which is consistent with our study. For example, the NCEP data have less total cloud fraction in the North Pacific during JJA than the ERA, yet the ERA has larger Q_{sw} than NCEP because of the high albedo of the NCEP clouds. It appears for stratiform cloud regimes that ERA has more realistic cloud albedos than NCEP, yet cloud fraction is still underestimated and results in the large positive bias.

Both ERA and NCEP underestimate Q_{sw} in regions where cumulus clouds are most common (Warren et al. 1988), with the ERA generally having a more negative bias. It appears compensating errors reduce the NCEP Q_{sw} bias in cumulus regimes; while the cloud albedos in the NCEP data are too large, the total cloud fraction is underestimated, resulting in smaller Q_{sw} biases than ERA. The ERA has strong negative biases ($< -40 \text{ W m}^{-2}$) in the tropical and subtropical regions where total cloud fraction bias is small ($< 10\%$, not shown). This indicates that water vapor absorption or cloud albedo may be the source of the negative Q_{sw} bias in cumulus regimes in the ERA.

Previous studies have shown that AGCMs and global reanalyses still have problems predicting clouds and cloud radiative properties. A typical comparative methodology of cloud radiative effects has been to look at annual mean and zonal mean biases, or land versus ocean biases. This can mask regional and seasonal biases at higher latitudes that may impact ocean models being forced with such flux estimates. Since the prediction of Q_{sw} is inherently linked to the prediction of clouds, AGCMs and global reanalyses will have limitations in Q_{sw} until better treatment of clouds is incorporated. Satellite estimates of Q_{sw} are preferable to model estimates because they begin with more accurate representations of clouds; however, they are limited in terms of their temporal duration. Observational efforts such as that of Moisan and Niiler (1998), which use both surface observations of clouds and satellite estimates of radiative fluxes to reconstruct radiative fluxes for years prior to satellite observations, may be our best estimates to date for use in forcing ocean model simulations for extended time periods.

Acknowledgments. The ERA and NCEP reanalysis data were provided by the NOAA/CIRES Climate Diagnostics Center, Boulder, Colorado (<http://www.cdc.noaa.gov/>). The satellite data were provided by the NASA/Langley Atmospheric Sciences Data Center (http://agni.larc.nasa.gov/SRB_homepage.html). Steve Worley at NCAR provided the mixed layer depth data. We thank Clara Deser and two anonymous reviewers for their comments which resulted in many improvements to the manuscript. This research was supported under NOAA Grant GC98-139.

REFERENCES

- Bony, S., Y. Sud, K. M. Lau, J. Susskind, and S. Saha, 1997: Comparison and satellite assessment of NASA/DAO and NCEP reanalyses over tropical ocean: Atmospheric hydrology and radiation. *J. Climate*, **10**, 1441–1462.
- Cess, R. D., and Coauthors, 1997: Comparison of the seasonal change in cloud-radiative forcing from atmospheric general circulation models and satellite observations. *J. Geophys. Res.*, **102**(D14), 16 593–16 603.
- Darnell, W. L., W. F. Staylor, S. K. Gupta, N. A. Ritchey, and A. C. Wilber, 1992: Seasonal variation of surface radiation budget derived from ISCCP-C1 data. *J. Geophys. Res.*, **97**, 15 741–15 760.

- ERA, 1999: The ECMWF Re-Analysis (ERA) Project. [Available online at <http://www.ecmwf.int/data/reanalysis.html>.]
- Garret, J. R., A. J. Prata, and L. D. Rotstayn, 1998: The surface radiation budget over oceans and continents. *J. Climate*, **11**, 1951–1968.
- Gupta, S. K., C. H. Whitlock, N. A. Ritchey, A. C. Wilber, W. L. Darnell, and W. F. Staylor, 1997: A climatology of surface radiation budget derived from satellite data. *Current Problems in Atmospheric Radiation*, W. L. Smith and K. Stamnes, Eds., A. Deepak, 1067 pp.
- Kalnay, E., and Coauthors, 1996: The NCEP/NCAR 40-Year Reanalysis Project. *Bull. Amer. Meteor. Soc.*, **77**, 437–471.
- Klein, S. A., and D. L. Hartmann, 1993: The seasonal cycle of low stratiform clouds. *J. Climate*, **6**, 1587–1606.
- , —, and J. R. Norris, 1995: On the relationships among low-cloud structure, sea surface temperature, and atmospheric circulation in the summertime northeast Pacific. *J. Climate*, **8**, 1140–1155.
- Li, Z., 1995: Intercomparison between two satellite-based products of net surface shortwave radiation. *J. Geophys. Res.*, **100**, 3221–3232.
- Liebmann, B., G. N. Kilidas, J. A. Marengo, T. Ambrizzi, and J. D. Glick, 1999: Submonthly convective variability over South America and the South Atlantic convergence zone. *J. Climate*, **12**, 1877–1891.
- Moisan, J. R., and P. P. Niiler, 1998: The seasonal heat budget of the North Pacific: Net heat flux and heat storage rates (1950–90). *J. Phys. Oceanogr.*, **28**, 401–421.
- Monterey, G. I., and S. Levitus, 1997: *Climatological Cycle of Mixed Layer Depth in the World Ocean*. NOAA NESDIS Atlas 14, U.S. Govt. Printing Office, 87 figs. plus 5 pp.
- Norris, J. R., and C. B. Leovy, 1994: Interannual variability in stratiform cloudiness and sea surface temperatures. *J. Climate*, **7**, 1915–1925.
- Ohmura, A., and H. Gilgen, 1991: The GEBA database: Interactive applications retrieving data (Heft 44). GEBA Rep. 2, Geographisches Institut, 66 pp. [Available from Prof. A. Ohmura, Geographisches Institut, ETH, Winterthurerstr. 190, CH-8057, Zurich, Switzerland.]
- Pinker, R. T., and I. Lazlo, 1992: Modeling surface solar irradiance for satellite applications on a global scale. *J. Appl. Meteor.*, **31**, 194 pp.
- Rossow, W. B., and Y.-C. Zhang 1995: Calculation of surface and top of atmosphere radiative fluxes from physical quantities based on ISCCP datasets. Part II: Validation and first results. *J. Geophys. Res.*, **100** (D1), 1167–1197.
- Schubert, S. D., J. Pfendner, and R. Rood, 1993. An assimilated dataset for earth science applications. *Bull. Amer. Meteor. Soc.*, **74**, 2331–2342.
- Snedecor, G. W., and W. G. Cochran, 1980: *Statistical Methods*. The Iowa State University Press, 507 pp.
- Ward, C. M., 1995: Comparison of the surface solar radiation budget derived from satellite data with that simulated by the NCAR CCM2. *J. Climate*, **8**, 2824–2842.
- Warren, S. G., C. J. Hahn, J. London, R. M. Chervin, and R. L. Jenne, 1988: Global distribution of total cloud cover and cloud type amounts over ocean. NCAR Tech. Note NCAR/TN-317+STR, National Center for Atmospheric Research, 42 pp. plus 170 maps.
- Weare, B. C., 1994: Interrelationships between cloud properties and sea surface temperatures on seasonal and interannual time scales. *J. Climate*, **7**, 248–260.
- , 1997: Comparison of NCEP-NCAR cloud radiative forcing reanalyses with observations. *J. Climate*, **10**, 2200–2209.
- Weaver, C. P., and V. Ramanathan, 1996: The link between summertime cloud radiative forcing and extratropical cyclones in the North Pacific. *J. Climate*, **9**, 2093–2109.
- Whitlock, C. H., and Coauthors, 1995: First global WCRP shortwave surface radiation budget dataset. *Bull. Amer. Meteor. Soc.*, **76**, 905–922.